

Preparation of ultrafine Co_3O_4 powders by continuous and controllable combustion synthesis

WU Chong-hu^{1,2}

1. China National R&D Center for Tungsten Technology, Xiamen Tungsten Co., Ltd. Technology Center, Xiamen 361009, China;
2. Xiamen Golden Egret Special Alloy Co., Ltd., Xiamen 361006, China

Received 9 November 2010; accepted 19 February 2011

Abstract: The continuously dynamic-controlled combustion synthesis (CDCCS) was developed based on the continuous fluidization and combustion synthesis technologies. $\text{CoC}_2\text{O}_4 \cdot 2\text{H}_2\text{O}$ powders were transformed to Co_3O_4 in a gas-solid fluid bed unit designed and build independently, where the reactant of $\text{CoC}_2\text{O}_4 \cdot 2\text{H}_2\text{O}$ powders and the reactant of air were poured and introduced from the top and the bottom of the bed at a certain rates respectively. The reagents met in the bed and ignited at a given low temperature, resulting in formation of Co_3O_4 . The results show a significant difference in combustion wave models. In the case of CDCCS, there was an immobile combustion wave, floating in the combustion zone located in the middle of the bed, instead of propagating of the combustion wave. The temperature of the combustion wave can be controlled by adjusting the flow rate of carrier gas. The resultant Co_3O_4 powders (diameter size $\leq 0.8 \mu\text{m}$) have a narrow particle size distribution and spherical or quasi-spherical shape. This novel technique has many advantages, such as continuation, efficiency, energy conservation and environmental friendly and has been used in mass production.

Key words: combustion synthesis; fluidization; cobalt oxide; ultrafine powders

1 Introduction

The ultrafine Co_3O_4 powders are important industrial raw materials. They can be used in the many areas including cemented carbides, battery materials[1], magnetic materials[2–3], catalysts[4], etc. The spherical or quasi-spherical ultrafine cobalt powders (diameter size $\leq 0.8 \mu\text{m}$) reduced from ultrafine Co_3O_4 powders are the key raw materials to produce ultrafine WC-Co cemented carbides. Conventionally, the cavernous cobalt powder with bar and dendrite morphology is mainly produced by hydrogen reduction of cobalt oxalate dehydrate ($\text{CoC}_2\text{O}_4 \cdot 2\text{H}_2\text{O}$) in the industrial electrical resistance tubular furnaces all over the world. There are frequently some coarse cobalt particles sized to several microns in final product so that it is difficult to fabricate high quality cemented carbides due to poor dispersibility, low flowability and microstructural inheritance. Furthermore, there is 2%–4% (mass fraction) hard agglomeration in cobalt powders always.

The oxide powders have been successfully

synthesized by the low temperature combustion synthesis (CS) using organometallic salts as precursors since the late 1980s[5]. At present, dozens of single oxide or composite oxide powders, including $\alpha\text{-Al}_2\text{O}_3$, mullite, ZnFe_2O_4 , Bi_2WO_6 , Li_2TiO_3 , $\text{YBa}_2\text{Cu}_3\text{O}_7$, $\text{Pr}_{0.8}\text{Sr}_{0.2}\text{Co}_{1-x}\text{Fe}_x\text{O}_3$, can be synthesized by this method[6–8]. The products obtained by CS have advantages of high purity, large surface area and good activity. However, the CS process should not be controlled due to the rapid reaction and the output of oxide products is low for the non-continuous process in the fixed bed or single layer fluidized bed.

The smoothly gas-solid fluidized bed and the bubbling gas-solid fluidized bed are in the fluidization stages, in which the bed particles are completely suspended by the air stream but do not meet the slugging fluidization. There are relative clear upper interfaces in these two fluidized beds, exhibiting liquid-like behavior. The liquid-like nature of these beds allows for high heat and mass transfer rates between the gas phase and the solid phase, and the particles can flow under gravity[9]. The two fluidized beds are collectively referred to as

boiling bed in the present work. Nitride powders such as TiN, TaN, CrN, have been produced by using the fluidized bed CS[10–11] and some progresses have been made. Nevertheless, the reactants cannot be converted completely and the method is non-continuous and uncontrollable. The fine SiO_2 , Si_3N_4 and TiC_xN_y powders were successfully produced via floating CS by ZHU[12]. The CS happened in fluidized bed and the powder was taken out from the furnace by pneumatic conveying. The next cycle of feeding raw materials, combustion synthesizing and discharging would be made only after all the powder products had been discharged from the furnace.

In the present study, the continuously dynamic-controlled combustion synthesis (CDCCS) process is proposed and the bottlenecks of continuous production and process controls of CS have also been solved satisfactorily. The energy-saving method and device for continuous formation of Co_3O_4 powder by combustion of $\text{CoC}_2\text{O}_4 \cdot 2\text{H}_2\text{O}$ were invented with the idea of CDCCS[13–14]. This method enriches the production practice of CS, which may also contribute to the research and application of CS theory. The principles of Co_3O_4 powder preparation by CDCCS were analyzed and described in means of thermodynamic analysis, process, morphology and application.

2 Experimental

The raw material of $\text{CoC}_2\text{O}_4 \cdot 2\text{H}_2\text{O}$ ($\text{Co} \geq 32.16\%$, mass fraction) was characterized by simultaneous thermogravimetric and differential thermal analysis instruments (Netzsch STA 409) in the flow of air (50 mL/min) with the heating rate of $5^\circ\text{C}/\text{min}$.

The preparation of Co_3O_4 powders via CDCCS was carried out in the gas-solid fluidized bed unit (CS unit), as shown in Fig.1. This unit is patented equipment that consists of fluidized bed roaster, feeding systems, receiving systems, dust collection systems and air supply system[13–14].

There is reaction and cooling boiling beds (11 and 21) that formed by gas-solid fluidization on the upper and lower gas distribution plates (61 and 62), respectively. The raw material on the upper gas distribution plate (61) is fleetly penetrated by the gas from upper gas pipeline (32). The boiling bed with the flowing property like liquid is formed when the superficial gas velocity reaches the critical value of 0.03 m/s. In our experiments, the superficial gas velocity was 0.09–0.18 m/s. The heights of boiling beds, existing between the gas distribution plates to the tops of overflow gates, were about 500 mm. And the thermocouples were installed on the CS unit' wall and the locations were about at 2/3 height of boiling beds, respectively.

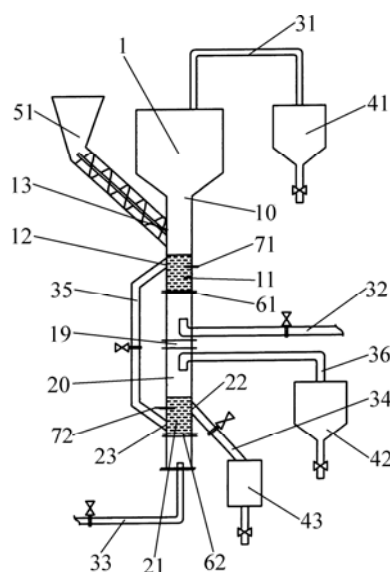


Fig.1 Schematic diagram of CS unit, in which Co_3O_4 powders prepared by CDCCS: 1—Fluidized bed roaster; 10—Upper chamber; 11—Reaction boiling bed; 12—Upper overflow gate; 13—Feed inlet; 19—Clapboard; 20—Lower chamber; 21—Cooling boiling bed; 22—Lower overflow gate; 23—Overflow entry; 31—Upper exhaust pipe; 32—Upper gas pipeline; 33—Lower gas pipeline; 34—Lower overflow pipe; 35—Upper overflow pipe; 36—Lower exhaust pipe; 41—Upper dust catcher; 42—Lower dust catcher; 43—Product collection container; 51—Screw feeder with storage hopper; 61—Upper gas distributor; 62—Lower gas distributor; 71—Upper thermocouple; 72—Lower thermocouple

When the boiling bed (11) containing $\text{CoC}_2\text{O}_4 \cdot 2\text{H}_2\text{O}$ that fed into by the screw feeder (51) was preheated to 380°C by the hot carrier gas, $\text{CoC}_2\text{O}_4 \cdot 2\text{H}_2\text{O}$ would react with O_2 in the air. The products of Co_3O_4 poured from upper overflow pipe (35) under gravity and entered into cooling boiling bed (21), followed by collecting from lower overflow pipe (34). The temperature of CS in reaction zone could be perfectly controlled through the linkage of the upper thermocouple (71) and the upper gas pipeline (32).

Once the CS reaction began, further heating does not needed due to the exothermic heat providing by the reaction of CoC_2O_4 converting into Co_3O_4 . The boiling bed provides the suitable circumstance for CS reaction with characters of continuous, dynamic and controllable. The morphology and particle size of the raw material and the resultant powders were observed by scanning electron microscope (SEM) (Hitachi S-3000N).

3 Results and discussion

3.1 Thermodynamic analysis

The results of TG-DTA curves for $\text{CoC}_2\text{O}_4 \cdot 2\text{H}_2\text{O}$ in

dynamic air are shown in Fig.2.

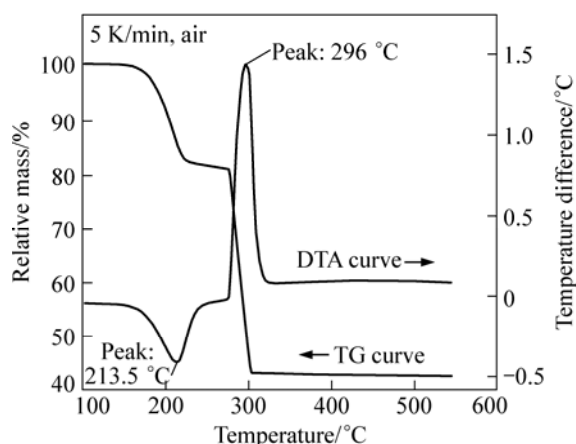
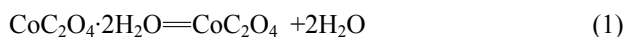


Fig.2 TG-DTA curves of $\text{CoC}_2\text{O}_4 \cdot 2\text{H}_2\text{O}$ in heating process

The endothermic peak on DTA curve appears at 213.5 °C, indicating that the dehydration reaction of $\text{CoC}_2\text{O}_4 \cdot 2\text{H}_2\text{O}$ occurs (see Eq.(1)). At 296 °C, an exothermic peak exists on DTA curve, suggesting that CoC_2O_4 reacts with O_2 in the air to form Co_3O_4 and releases large amount of heat (see Eq.(2)).



The $\text{CoC}_2\text{O}_4 \cdot 2\text{H}_2\text{O}$ was heated in the flow of air (30 mL/min) with the heating rate of 2, 5, 10 and 20 °C/min, respectively, by MANSOUR[15]. The endothermic peak occurred at 170–225 °C and the exothermic peak of oxidation reaction occurred at 275–300 °C. The temperatures of peaks on DTA curves increased with the increase of heating rate. The $\text{CoC}_2\text{O}_4 \cdot 2\text{H}_2\text{O}$ was heated in the flow of air (100 mL/min) with the heating rate of 10 °C/min, and the endothermic peak of dehydration reaction and the exothermic peak of oxidation reaction occurred at 198 °C and 311 °C[16], respectively. In addition, the product of Co_3O_4 could only stably exist at 890 °C. The $\text{CoC}_2\text{O}_4 \cdot 2\text{H}_2\text{O}$ was heated in static air with the heating rate of 3 °C/min, and the endothermic peak of dehydration reaction and the exothermic peak of oxidation reaction occurred at 193 °C and 320 °C[17], respectively. The thermogravimetric kinetic analysis of $\text{CoC}_2\text{O}_4 \cdot 2\text{H}_2\text{O}$ was also carried out on a Netzsch STA 409 thermal analyzer in the exact flow of He+20% (volume fraction) O_2 (100 mL/min) with the heating rate of 10 °C/min[18], and the endothermic peak and the exothermic peak on the DSC curve occurred at 199 °C and 279 °C, respectively.

It can be concluded from the results of thermal analysis that the dehydration reaction of $\text{CoC}_2\text{O}_4 \cdot 2\text{H}_2\text{O}$ occurs at 170–225 °C and the oxidation reaction occurs at 275–320 °C in oxidizing atmosphere[15–18]. The CoC_2O_4 has converted completely to Co_3O_4 at

temperature higher than 320 °C. Moreover, the dehydration reaction of $\text{CoC}_2\text{O}_4 \cdot 2\text{H}_2\text{O}$ and the oxidation reaction of CoC_2O_4 are performed rapidly and completely. Therefore, the combustion temperature was set at 380–400 °C in our experiments.

At present, the thermodynamic data of $\text{CoC}_2\text{O}_4 \cdot 2\text{H}_2\text{O}$ and CoC_2O_4 in the adiabatic state are hardly available and several thermodynamic databases do not contain these data. Several groups of adiabatic thermodynamic data of $\text{CoC}_2\text{O}_4 \cdot 2\text{H}_2\text{O}$ and CoC_2O_4 were given in Ref.[18]. Nevertheless, there are large differences without comparability due to the different experimental conditions. Here, the thermodynamic data in Ref.[15] were used to calculate Eq.(3) because they were tested under the same condition. We have

$$\Delta H_1 + \Delta H_2 + n \int_{298.15}^{673.15} c_p = 0 \quad (3)$$

where ΔH_1 and ΔH_2 are enthalpies of Eq.(1) and Eq.(2), respectively; n is the number of moles (mol) and c_p is the average heat capacity of $\text{CoC}_2\text{O}_4 \cdot 2\text{H}_2\text{O}$.

Suppose the composition and structure of $\text{CoC}_2\text{O}_4 \cdot 2\text{H}_2\text{O}$ do not change at 25–400 °C and c_p is the average heat capacity, and then $n=6.5$ in Eq.(3). It is indicated that the quantity of heat released by combustion of 1 mol $\text{CoC}_2\text{O}_4 \cdot 2\text{H}_2\text{O}$ in the air can raise the temperature of 6.5 mol $\text{CoC}_2\text{O}_4 \cdot 2\text{H}_2\text{O}$ from 25 °C to 400 °C. If only 1 mol $\text{CoC}_2\text{O}_4 \cdot 2\text{H}_2\text{O}$ was heated from 25 °C to 400 °C, then the rest energy (~29 kJ) should release to the environment. The suitable preparation conditions of Co_3O_4 powder by CS can meet thanks to the strongly exothermic reaction.

3.2 Process analysis of CDCCS for Co_3O_4 powders

As the reactant powders of $\text{CoC}_2\text{O}_4 \cdot 2\text{H}_2\text{O}$ fell down to combustion zone in the boiling bed, no self sustaining reaction occurred. Only when the whole $\text{CoC}_2\text{O}_4 \cdot 2\text{H}_2\text{O}$ powders entranced the combustion zone and were heated by hot carrier gas the sustaining reaction was ignited. This means that once the combustion reaction between O_2 and $\text{CoC}_2\text{O}_4 \cdot 2\text{H}_2\text{O}$ is ignited, the heat produced by combustion reaction will be used to ignite the following exothermic reaction and no external heat is needed, then the hot carrier will be transformed into the cool carrier gas.

Fig.3 shows the temperatures of combustion wave and its relationship with the superficial gas velocity and feeding rate of $\text{CoC}_2\text{O}_4 \cdot 2\text{H}_2\text{O}$ during the stable combustion synthesis. When the feeding rate does not change, the temperature of combustion wave declines with increasing gas velocity; and when gas velocity does not change, the temperature of combustion wave increases with increasing the feeding rate. According to Fig.3, the temperature of combustion wave could be adjusted dynamically by changing the feeding rate of raw

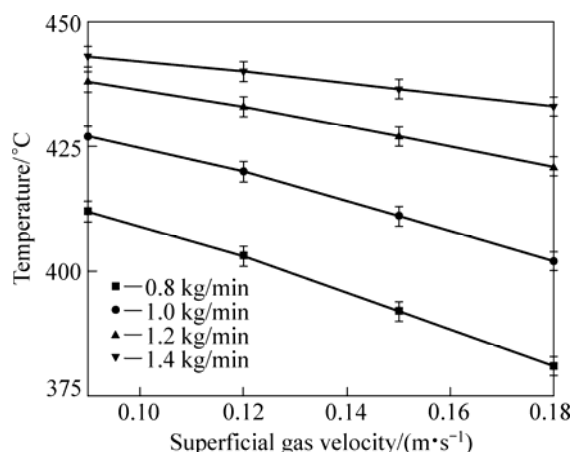


Fig.3 Temperature curves of combustion wave with different feeding rates and superficial gas velocities in boiling bed

material and/or the superficial gas velocity.

Different from conventional CS, the combustion wave here was almost full of the combustion zone in the middle of the boiling bed and the temperatures in a three-dimensional space were homogeneous, as shown schematically at the small arrows in Fig.4. The combustion wave was relatively suspended in the fluidized bed. Moreover, the temperature in the combustion zone could be dynamically controlled by adjusting the flow of carrier gas, as mentioned above. During the preparation, the powders of $\text{CoC}_2\text{O}_4 \cdot 2\text{H}_2\text{O}$ were fed by the screw feeder into the upper area of reaction boiling bed and contacted with the combustion wave. After the CS, the products of Co_3O_4 powders fell down and left the combustion wave in time through flowing out off the overflow gate on the wall of the unit continuously.

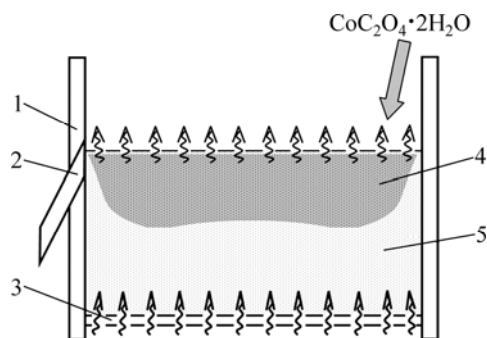


Fig.4 Schematic diagram of combustion zone in reaction boiling bed: 1—Furnace wall; 2—Overflow gate; 3—Gas distributor; 4—Boiling bed; 5—Combustion zone

The CS unit in the present work is different from conventional one also[19]. In the conventional unit, the reactants and products are nearly stationary while the combustion wave propagates from reactants to products. Our unit combined with advantages of the technologies

of continuous fluidization and CS. The combustion wave was relatively stationary, but the reactants and products were mobile at a given speed.

The novel method has several advantages: 1) Co_3O_4 powder was successfully produced in the fluidized bed unit and the production efficiency was improved; 2) No external heat was needed when the reaction was ignited, therefore, the energy consumption was reduced; 3) The materials flowed in a closed unit so that clean operation and cleaner product were realized; 4) the device operations were automated, except the transport of reactants and products, thus it reduced labor intensity.

The preparation of ultrafine Co_3O_4 powders (diameter size $\leq 0.8 \mu\text{m}$) by continuous and controllable combustion synthesis has been successfully applied in Xiamen Golden Egret Special Alloy Co., Ltd[13–14]. And the production capacity of fine or ultrafine Co_3O_4 powders produced by this method has reached 500 t/a.

3.3 Morphology of ultrafine Co_3O_4 powders

Fig.5(a) shows that the short strip particles of $\text{CoC}_2\text{O}_4 \cdot 2\text{H}_2\text{O}$ with the average length below $6 \mu\text{m}$ stack disorderly. In conventional production method, the Co_3O_4 powders by directly hydrogen reduction from $\text{CoC}_2\text{O}_4 \cdot 2\text{H}_2\text{O}$ in fixed bed of the electrical resistance tubular furnaces are in a narrow strip shape. These powders weave together and have coarse grains with a wide particle size distribution (see Fig.5(b)). Worse still, there is Fischer-Tropsch exothermic reaction in this conventional fixed bed method[20]. The exothermic reaction can lead to sintering between some touching Co powders and having 2%–4% hard agglomeration of the total mass.

When these particles of $\text{CoC}_2\text{O}_4 \cdot 2\text{H}_2\text{O}$ have been converted into Co_3O_4 powders in boiling bed, the particles were transformed from jagged or serrated shape into hemispherical, and every short strip particle also was decomposed spherical or quasi-spherical particles (see Fig.5(c)). In the gas-solid fluidized bed unit, the temperature of the whole boiling bed is nearly homogeneous and the suspended solid particles collide with each other without aggregation[21], and hence almost each solid particle in the boiling bed has a similar surrounding. All the $\text{CoC}_2\text{O}_4 \cdot 2\text{H}_2\text{O}$ particles contact and react with O_2 completely. The uneven distributions of particle size or hard aggregation appear scarcely due to the favorable diffusion condition and rapid transfer of heat and mass. The Co_3O_4 powders produced with the industrial unit schematically shown in Fig.2 possess the narrow particle size distribution, good dispersions and excellent flowing property.

The hydrogen reduced ultrafine Co powders using fine or ultrafine Co_3O_4 powders produced by CS as raw materials are spherical or quasi-spherical also. These

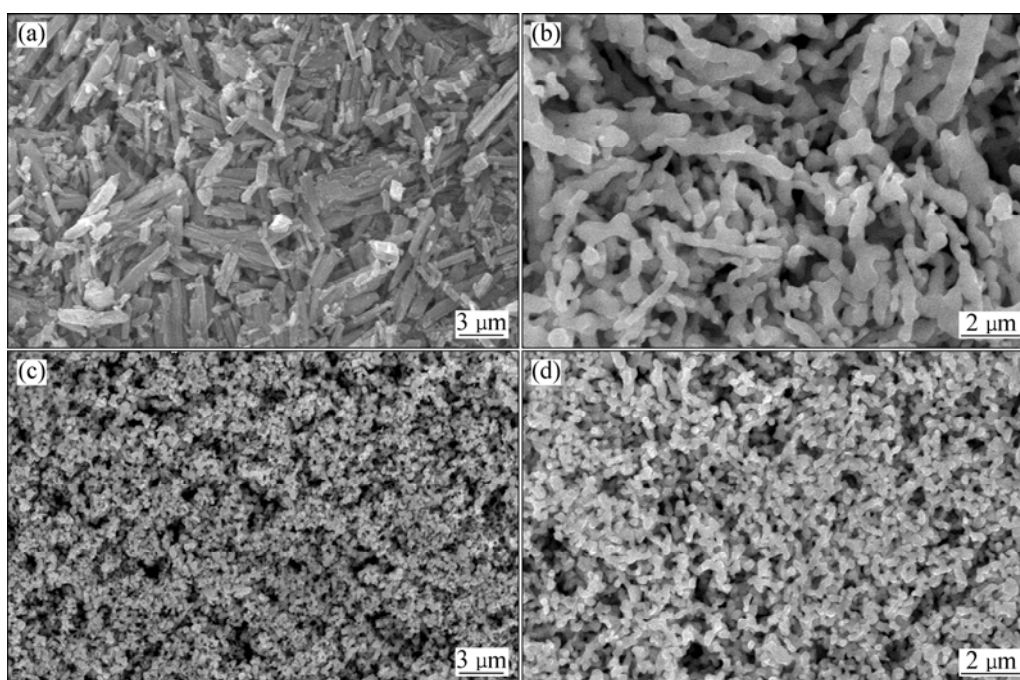


Fig.5 SEM images of samples: (a) $\text{CoC}_2\text{O}_4 \cdot 2\text{H}_2\text{O}$ powders; (b) Dendritic Co_3O_4 powders; (c) Co_3O_4 ultrafine powders; (d) Co_3O_4 powders with quasi-spherical shape

powders with an average size of $0.6 \mu\text{m}$ possess a narrow particle size distribution (see Fig.5(d)). From Fig.5(c) and Fig.5(d), it can be seen that the production process of Co_3O_4 powder by the CDCCS possesses excellent product quality.

4 Conclusions

1) The reaction between CoC_2O_4 and O_2 in the air is a strongly exothermic reaction. The heat produced by this oxidation reaction can be used to ignite the following reaction at $400 \text{ }^\circ\text{C}$.

2) The CDCCS combines with the technologies of gas-solid fluidization and CS. The tranquil combustion wave is located in boiling bed after the reactants are ignited, the following reactants are fed into boiling bed and contact with the combustion wave at a given speed and the products are taken away from boiling bed continuously under gravity. The temperature of combustion wave can be controlled by adjusting the amount of the flow carrier gas.

3) The ultrafine Co_3O_4 powders (diameter size $\leq 0.8 \mu\text{m}$) with narrow particle size distributions are produced by the continuous and controllable combustion synthesis in the gas-solid fluidized bed unit using the strongly exothermic reaction of CoC_2O_4 in air. This production process is based on the technology of CDCCS and shows many advantages, such as continuation, controllable and energy conservation.

References

- [1] LU Yan, WANG Yong, ZOU Yu-qin, ZHENG Jiao, ZHAO Bing, HE Ya-qin, WU Ming-hong. Macroporous Co_3O_4 platelets with excellent rate capability as anodes for lithium ion batteries [J]. *Electrochemistry Communications*, 2010, 12(1): 101–105.
- [2] LIU Yan, ZHANG Xiao-gang. Effect of calcination temperature on the morphology and electrochemical properties of Co_3O_4 for lithium-ion battery [J]. *Electrochimica Acta*, 2009, 54(17): 4180–4185.
- [3] DONG Zhao, XU Ying-ying, ZHANG Xiong-jian, JIN Wen-tao, KASHKAROV P, ZHANG Han. Novel magnetic properties of Co_3O_4 nanowires [J]. *Solid State Communications*, 2009, 149(15–16): 648–651.
- [4] XIA Yun-sheng, DAI Hong-xing, JIANG Hai-yan, ZHANG Lei. Three-dimensional ordered mesoporous cobalt oxides: Highly active catalysts for the oxidation of toluene and methanol [J]. *Catalysis Communications*, 2010, 11(15): 1171–1175.
- [5] KINGSLEY J J, PATIL K C. A novel combustion process for the synthesis of fine particle α -aluminum and related oxide materials [J]. *Materials Letters*, 1988, 6(11–12): 427–432.
- [6] LI Wen-xia, YIN Sheng. Low temperature combustion synthesis of ultrafine ceramic powder [J]. *Journal of the Chinese Ceramic Society*, 1999, 27(1): 71–78. (in Chinese)
- [7] ZHANG Zhi-jie, WANG Wen-zhong, SHANG Meng, YIN Wen-zong. Low-temperature combustion synthesis of Bi_2WO_6 nanoparticles as a visible-light-driven photocatalyst [J]. *Journal of Hazardous Materials*, 2010, 177(1–3): 1013–1018.
- [8] MAGNONE E, TRAVERSA E, MIYAYAMA M. Nano-sized $\text{Pr}_{0.8}\text{Sr}_{0.2}\text{Co}_{1-x}\text{Fe}_x\text{O}_3$ powders prepared by single-step combustion synthesis for solid oxide fuel cell cathodes [J]. *Journal of Electroceramics*, 2010, 24(2): 122–135.
- [9] WU Zhan-song, MA Run-tian, WANG Zhan-wen. Fluidization

- technology basis and applications [M]. Beijing: Chemical Industry Press, 2006: 3–9. (in Chinese)
- [10] JAIN A, BREZINSKY K. Microwave-assisted combustion synthesis of tantalum nitride in a fluidized bed [J]. *Journal of the American Ceramic Society*, 2003, 86(2): 222–226.
- [11] LEE K O, COHEN J J, BREZINSKY K. Fluidized-bed combustion synthesis of titanium nitride [J]. *Proceedings of the Combustion Institute*, 2000, 28(1): 1373–1380.
- [12] ZHU Yuan, JIN Hai-bo, REN Ke-gang, AGATHOPOULOS S, CHEN Ke-xin. Floating combustion synthesis of spherical vitreous silica nano-powder [J]. *Materials Research Bulletin*, 2009, 44(1): 130–133.
- [13] WU Chong-hu. Energy-saving method and device for continuous production of tricobalt tetraoxide by cobaltous oxalate: CN 101062791 [P]. 2007–10–31. (in Chinese)
- [14] WU Chong-hu. Energy saving type device for continuously producing Co_3O_4 by cobalt oxalate: CN 2900494 [P]. 2007–05–16. (in Chinese)
- [15] MANSOUR S A A. Spectrothermal studies on the decomposition course of cobalt oxsalts. Part III. Cobalt oxalate dehydrate [J]. *Materials Chemistry and Physics*, 1994, 36(3–4): 324–331.
- [16] TIAN Qing-hua, GUO Xue-yi, LI Jun. Thermodynamic analysis and thermal decomposition behavior of cobalt oxalate [J]. *Mining and Metallurgical Engineering*, 2009, 29(4): 67–69, 73. (in Chinese)
- [17] ZHANG Jian-jun, REN Ning, BAI Ji-hai. Non-isothermal kinetics of the first-stage decomposition reaction of cobalt oxalate dehydrate [J]. *Chemical Research in Chinese Universities*, 2005, 21(4): 501–504.
- [18] MACIEJEWSKI M, INGIER-STOCKA E, EMMERICH W D, BAIKER A. Thermal decomposition of cobalt oxalate dehydrate [J]. *Journal of Thermal Analysis and Calorimetry*, 2000, 60: 735–758.
- [19] YIN Sheng. Combustion synthesis [M]. Beijing: Metallurgical Industry Press, 2004: 436–438. (in Chinese)
- [20] MAJUMDAR S, SHARMA I G, BIDAYE A C, SURI A K. A study on isothermal kinetics of thermal decomposition of cobalt oxalate to cobalt [J]. *Thermochimica Acta*, 2008, 473(1–2): 45–49.
- [21] SAXENA S C, RAO N S, THOMAS L A. Combustion of propane and fluidized-bed co-combustion [J]. *Energy*, 1993, 18(10): 1045–1057.

连续和可控的燃烧法合成 Co_3O_4 超细粉

吴冲浒^{1,2}

1. 国家钨材料工程技术研究中心 厦门钨业股份有限公司技术中心, 厦门 361009;
2. 厦门金鹭特种合金有限公司, 厦门 361006

摘要: 结合气固流态化和燃烧合成理论, 提出连续动态可控燃烧合成概念。在自主设计、制作的气固流态床设备中, 将 $\text{CoC}_2\text{O}_4 \cdot 2\text{H}_2\text{O}$ 制备成 Co_3O_4 。反应物 $\text{CoC}_2\text{O}_4 \cdot 2\text{H}_2\text{O}$ 粉体和空气分别以一定的速度被从沸腾床的上部加入和底部引入。 $\text{CoC}_2\text{O}_4 \cdot 2\text{H}_2\text{O}$ 和空气在床层中相遇, 并在给定的低温下被点燃并合成 Co_3O_4 。结果表明: 燃烧波模式与传统燃烧合成燃烧波的不同, 在连续动态可控燃烧合成中, 燃烧波位置相对不动, 悬浮在沸腾床中部的燃烧区域, 而不是移动的自蔓延燃烧波; 燃烧波温度可以通过改变载气流速、流量进行调节; 产物 Co_3O_4 粉末 ($\leq 0.8 \mu\text{m}$) 呈球形或准球形, 粒度分布均匀。本方法具有连续高效、节能环保的优点, 已经应用于大规模生产。

关键词: 燃烧合成; 流态化; Co_3O_4 ; 超细粉末

(Edited by YANG Hua)